Biophysical Chemistry 42 (1992) 49–61
Elsevier Science Publishers B.V., Amsterdam

BIOCHE 01597

Selective laser spectroscopy of 1-phenylnaphthylamine in phospholipid membranes

Dmitry M. Gakamsky [a], Alexander P. Demchenko [b], Nikolay A. Nemkovich [a], Anatoly N. Rubinov [a], Vladimir I. Tomin [a] and Nina V. Shcherbatska [b]

[a] *Institute of Physics, Academy of Sciences of Byelarus SSR, 220602-Minsk (Byelorussia)*
[b] *Institute of Biochemistry, Academy of Sciences of Ukrainian SSR, 252030-Kiev (Ukraine)*

(Received 22 July 1988; accepted in revised form 16 April 1991)

Abstract

Time-resolved and steady-state spectra and kinetics of anisotropy of 1-phenylnaphthylamine (1-AN) fluorescent probe in phosphatidylcholine bilayer membranes have been examined using a nanosecond laser spectrofluorimeter. In this system we consider two kinds of inhomogeneous broadening of spectra, the first of which is due to different probe locations in membrane, while the second one is due to the statistical distribution of interaction energy within a given location. This broadening causes the red shift of the fluorescence spectrum at red-edge excitation, the specific dependences of instantaneous fluorescence and fluorescence anisotropy spectra on the wavelength of excitation. A field diagram is presented which, by describing the free energy levels of the polar fluorescent probe in membranes, makes it possible to unambiguously interpret the whole set of experimental data. It is suggested that the release of potential energy of intermolecular interactions which occurs in the process of relaxation, results in accelerated (light-induced) rotation of the probe inside the membrane.

Keywords: Phospholipid membranes; Fluorescent probe; Red-edge excitation fluorescence shift; Time-resolved spectroscopy; Time-resolved anisotropy; Subnanosecond and nanosecond mobility; Inhomogeneous broadening

1. Introduction

To understand the elementary mechanisms of complicated processes associated with realization of the numerous functions of biological membranes, one needs detailed information not only about their molecular structure, but also about their structural dynamics. The purpose of these studies is to elucidate the types and characteristic times of motions of the molecules and their segments in the membrane. The advent of new experimental facilities which make it possible to achieve a high (subnanosecond and nanosecond) time resolution, have spurred a new tide of interest in the well-known method of fluorescent probes [1–3]. The data that can be obtained by means of kinetic fluorescence spectroscopy is especially valuable, since this method permits direct observation of the dynamics of various processes in the condensed media, such as configurational relaxation of dipole molecules, electronic excitation energy transfer, Brownian rotation, various photochemical reactions, etc. Besides, it provides ways to discriminate between the contributions

made by the processes which occur at different rates and the superposition of which results in a complicated pattern of time-integrated fluorescent characteristics.

Aminonaphthalenes [1,4,5] are being widely used as fluorescent probes in studies of model and natural membranes. The sensitivity of the fluorescence parameters of these probes to structural dynamics of their environment is due to their important property, i.e. the considerable change of their dipole moment at the time of electronic excitation. The fluorescence spectra of these probes depend substantially on the polarity of the environment and its capability of changing orientation during the lifetime of electronic excited state, which is the result of the substantial influence of dipole–dipole interactions with the environment on their characteristics [6]. The 1.8-ANS(1-anilinonaphthalene-8-sulfonate) and 2.6-TNS 2-toluidinonaphthalene-6-sulfonate are the amphiphilic probes whose spectral properties and localizations in membrane have been studied in the most extensive way. Owing to the presence of a negatively charged sulphate group, they located in the region of the heads of phospholipids at the polar surface layer of the membrane phospholipid bilayer. As shown by Demchenko and Shcherbatska [7], in these cases configurational relaxation in the system, which includes probe and its immediate environment, occurs in sub-nanosecond and nanosecond time domain.

The question arises: how high is the mobility of lipid segments and probe molecules in the deeper locations of the bilayer? Phenylnaphthylamines, 1-AN and 2-AN, are among the probes enabling the study of the membrane areas located deeper than the phospholipid heads [1,5,8]. Since no charge is present in these probes, their location corresponds to the level of the glycerol skeleton and carbonyl group of phospholipids [9,10]. The bonds between the probe molecules and these groups are characterized by the magnitude of the association constants, which are of the order of 10^4–10^5 M^{-1} [11].

The study of the decay curves of fluorescence intensity, anisotropy and time-resolved fluorescence spectra [12] proved the existence of nanosecond dynamics of 2-AN in lecithin liposomes. However, this study did not specify the mechanism of probe rotation. It was assumed that it was essentially the equilibrium Brownian diffusion. In a more recent study [9], the spectral kinetics of 1-AN was observed by using the method of phase fluorometry. Several of the latest publications [13,14] have provided illustrations of the heterogeneous character of fluorophore incorporation into the bilayer.

In the present paper the fluorescence and polarization (steady-state and time-resolved) characteristics of a 1-AN fluorescent probe in phosphatidylcholine bilayer membranes have been examined using a nanosecond laser spectrofluorimeter. It is shown that the electronic spectra of 1-AN in membranes are inhomogeneously broadened. This is confirmed by the red-edge excitation shift of the steady-state fluorescence spectra, the time-dependent fluorescence shift (TDFS) and by their temperature dependencies. The obtained results proves the existence of the earlier unknown effect of the light-induced rotation of the probe in membranes. This rotation exceeds the equilibrium Brownian one and occurs due to the release of intermolecular interactions potential energy during the relaxation. The free energy diagram is presented which describes the probe molecule's configurational sublevels.

2. Materials and methods

The experiments were carried out with vesicles obtained by the conventional method from egg yolk phosphatidylcholine [15]. Vesicles were produced by short-term (10–15 min) sonication of lipid suspension in 50 mM tris-HCl buffer, pH 7.4, using a 150-Watt ultrasonic disintegrator (MSE). The conditions for experiment were chosen to provide the predominant formation of bilayer monolamellar vesicles. The vesicles were separated by size with a centrifuge and additionally fractioned in Sepharose 4B. The final lipid concentration and the vesicle size were determined as described in [16]. Experiments were

carried out with vesicles of sizes ranging from 100 nm to 200 nm, at a lipid concentration equal to 10 mg/ml.

A probe dissolved in ethanol was added to lecithin in the chloroform–methanol system prior to drying and sonic treatment. In the experiments with fluorescence excitation at the maximum of absorption the lipid–probe ratio was 1000 : 1 while at the red-edge excitation the corresponding value was close to be 500 : 1. As was shown by preliminary studies, higher probe concentrations led to distorted fluorescence spectra and to a decrease in fluorescence polarization due to the nonradiative energy transfer. When experiments were conducted at low temperatures, a 60% (w/v) sucrose solution was added to the vesicles suspension (its final concentration was not to exceed 20%). The spectral characteristics of vesicles at 0 °C with and without sucrose were identical.

The probe 1-AN of chromatographic purity was synthesized at the Institute of Organic Chemistry of the Ukrainian Academy of Sciences, Kiev.

The steady-state fluorescence spectra were recorded on MPF-4 spectrofluorimeter (Hitachi, Japan). The spectra of 1-AN in ethanol were in accord with the literature data [17]. The background (vesicles suspension without probe) was subtracted from the corresponding fluorescence spectra. The quartz cell was thermostabilized by circulating of water or of a ethanol/water mixture using the UTU-3 ultra thermostat (Poland) or the MK-70 cryothermostat (Germany). Steady-state polarization measurements were carried out by means of MPF-4 in which polaroid films were additionally installed.

To investigate the spectral kinetics and rotational dynamics of the probe in the phospholipid membrane, a nanosecond laser spectrofluorimeter [18] was used. The recording system can measure four fluorescent characteristics: (i) the kinetics of fluorescence decay at any wavelength of excitation and emission, (ii) the kinetics of emission anisotropy at any wavelength of excitation and emission, (iii) time-resolved emission spectra, and (iv) time-resolved spectra of emission anisotropy.

The subsequent processing of data was carried out by means of a computer system.

The kinetics of emission anisotropy was calculated using the well-known formula:

$$r(t) = \left((I^{\parallel}(t) - I^{\perp}(t))/(I^{\parallel}(t) + 2I^{\perp}(t))\right),$$

where $I^{\parallel}(t)$ and $I^{\perp}(t)$ are emission components polarized in parallel and perpendicular to the direction of light excitation polarization respectively.

3. Results

3.1 Red-edge excitation fluorescence effects in the steady-state spectra

The red-edge excitation fluorescence effect (REEFE) is a general spectroscopic phenomenon observable in the case of inhomogeneously broadened spectra and slow (with respect to the fluorescence lifetime) dipole relaxation of the chromophore environment. When fluorescence is excited at the red edge of the absorption band, the fluorescence spectrum is shifted towards a longer wavelength.

The results obtained for 1-AN in viscous and solid solutions (Fig. 1) demonstrate a substantial

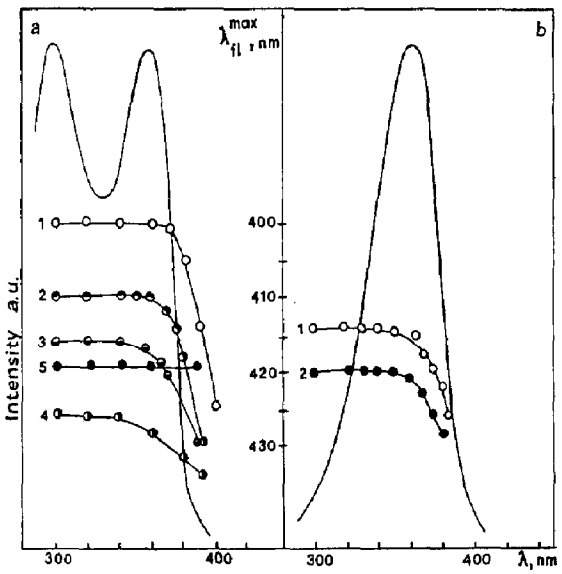

Fig. 1. The maxima of the fluorescence spectra of 1-AN as the function of the excitation wavelength. (a) 1 – In polymethylmethacrylate film; 2,3,4 – in glycerol at temperatures −15 °C, 1 °C, 35 °C, respectively, and 5 – in ethanol, 20 °C. (b) In phosphatidylcholine vesicles: 1–1 °C, 2–25 °C. The solid line represents the excitation spectrum.

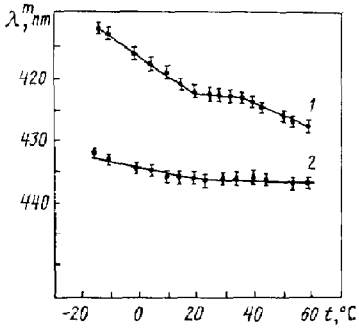

Fig. 2. The temperature dependence of the maxima of the fluorescence spectra of 1-AN in phosphatidylcholine vesicles. Excitation wavelengths: 360 nm (1) and 390 nm (2).

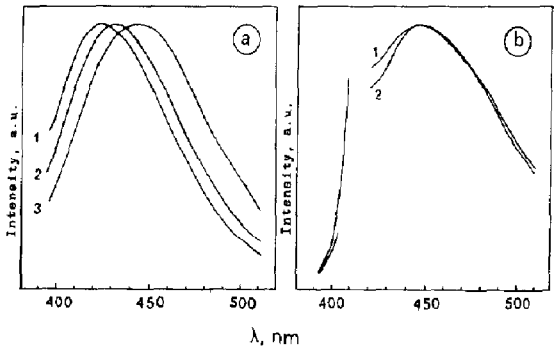

Fig. 3. The time-resolved fluorescence spectra of 1-AN in glycerol at different excitation wavelengths. (a) $\lambda_{ex} = 337$ nm: 1–2 ns, 2–3 ns, and 3–14 ns after excitation. (b) $\lambda_{ex} = 416$ nm: 1–2 ns, and 2–8 ns after excitation.

shift of fluorescence spectra at the transition of excitation to the absorption bond red edge. As it was expected, the REEFE was absent in a liquid solution. This effect considerably decreased when the solution of 1-AN in glycerol was heated. The long-wavelength shift of steady-state emission spectrum occurring with the decreasing of excitation frequency was not accompanied by any noticeable change of its shape. The isosbestic point was also absent, which proves that the observed phenomenon cannot be explained by photochemical transition of the emitting center to some other form, but rather correspond to the continuous reconstruction of the fluorescence center in accordance with the the model of continuous spectral relaxation. In experiments with 1-AN in vesicles the REEFE was well pronounced and revealed a considerable temperature dependence.

We have studied the temperature dependence of position of 1-AN fluorescence maximum in vesicles at two excitation wavelengths (at the longwave absorption band maximum, 360 nm and at its edge, 390 nm) (Fig. 2). It is seen from Fig. 2 that one can distinguish two temperature regions of spectral shifts: from $-20\,^{\circ}C$ to $20\,^{\circ}C$ and from $40\,^{\circ}C$ to $60\,^{\circ}C$. Within the 20–40 °C range, 1-AN fluorescence spectra are practically temperature-independent.

3.2 Nanosecond time-resolved fluorescence spectra of 1-AN in vesicles and solutions

The time-resolved fluorescence spectra of 1-AN in glycerol and in vesicles at two excitation wavelengths (the excitation at the maximum of (a) the absorption band and (b) the red-edge excitation are shown in Figs. 3 and 4. The shape of time-resolved spectra at both excitation wavelengths does not reveal any substantial changes with time during the relaxation. Figure 5 shows the positions of the time-resolved fluorescence spectral maxima of 1-AN in glycerol (a) and in vesicles (b) as a function of time for different excitation wavelengths. At red-edge excitation the magnitude of the spectral relaxation decreases for both systems, but for 1-AN in glycerol the time-resolved spectra at different excitation wavelengths tend to the same position while in vesicles they tend to different positions. The spectral kinetics of the probe in glycerol solution disappears at the excitation wavelength of 416

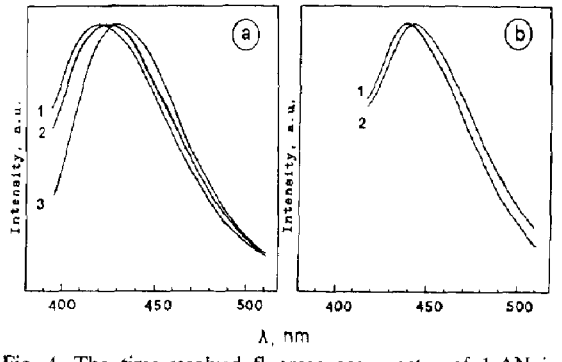

Fig. 4. The time-resolved fluorescence spectra of 1-AN in phosphatidylcholine vesicles at different excitation wavelengths. (a) $\lambda_{ex} = 337$ nm: 1–2 ns, 2–3 ns, and 3–14 ns after excitation. (b) $\lambda_{ex} = 390$ nm: 1–3 ns, and 2–8 ns after excitation.

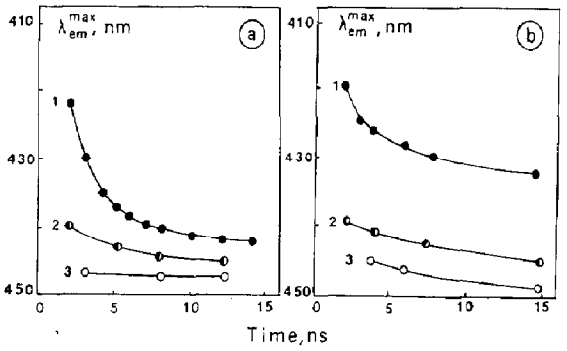

Fig. 5. The dependence of the maxima of time-resolved fluorescence spectra on the registration time for 1-AN in phosphatidylcholine vesicles (a) and in glycerol (b) at different excitation wavelengths. (a) Curves 1, 2, 3– at $\lambda_{ex} = 337$ nm, 400 nm, and 416 nm, respectively. (b) Curves 1, 2, 3–at $\lambda_{ex} = 337$ nm, 390 nm, and 410 nm, respectively.

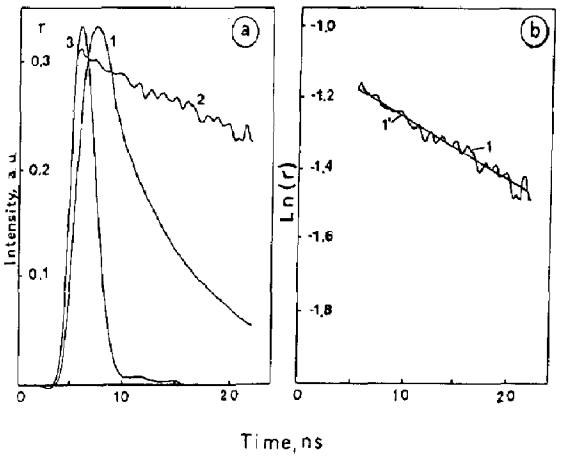

Fig. 6. Kinetics of anisotropy of 1-AN in glycerol at 22 °C (excitation wavelength 337 nm). (a) The kinetics of fluorescence (1), emission anisotropy (2) and the excitation pulse (3). (b) The kinetics of emission anisotropy in the semilogarithmical scale (1) and its approximation (1) by the least-squares method.

nm. It is interesting to note that the temporal shift of the fluorescence spectra of 1-AN in vesicles did not disappear at the excitation wavelength up to 410 nm, the longest wavelength, which could be used in our experiment. The registration of probe fluorescence at the excitation wavelengths greater than 410 nm was not possible because of the intensive light scattering in membrane suspension.

3.3 Spectral and temporal characteristics of 1-AN fluorescence anisotropy

The nanosecond time dependence of emission anisotropy of 1-AN in glycerol was measured at the excitation wavelength 337 nm (Fig. 6). Within experimental error the kinetics of anisotropy was monoexponential with a characteristic time 63 ± 4 ns. As seen from Fig. 6, the emission anisotropy at the initial moment is close to the limiting value $r_0 = 0.3$. According to our measurements this value will stay constant along the long-wavelength absorption band. Also, we have not found any dependence of the nanosecond kinetics of emission anisotropy of 1-AN in glycerol on the emission wavelength.

On the other hand, the decay of emission anisotropy of 1-AN in lecithin vesicles are non-exponential and depends on the excitation and emission wavelengths (Figs. 7 and 8). The anisotropy kinetics at the excitation wavelength 337 nm ("blue" excitation) reveals a fast sub-nanosecond part (see Fig. 7). We were unable to record its initial stage due to the limiting time resolution of our setup. The presence of this fast component of fluorescence depolarization is indi-

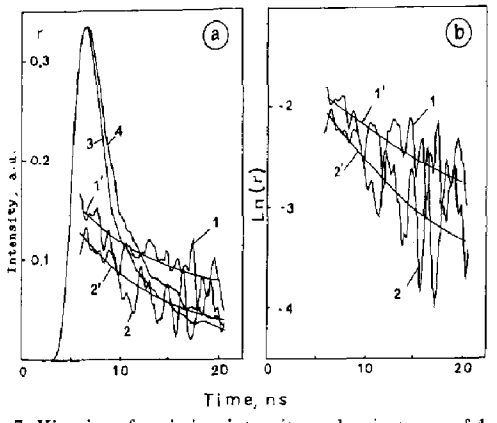

Fig. 7. Kinetics of emission intensity and anisotropy of 1-AN in phosphatidylcholine vesicles at 22 °C (excitation wavelength 337 nm). (a) The kinetics of anisotropy registered on the blue (430 nm, curve 1) and the red (485 nm, curve 2) slope of the fluorescence spectrum and its approximation by the least-squares method (curves 1 and 2). Curves 3 and 4 are the kinetics of fluorescence emission registered at the wavelength 430 nm and 485 nm, respectively. (b) The kinetics of emission anisotropy in the semilogarithmical scale registered at the wavelength 430 nm (curve 1) and 485 nm (curve 2) and its approximation (1', 2') by the least-squares method.

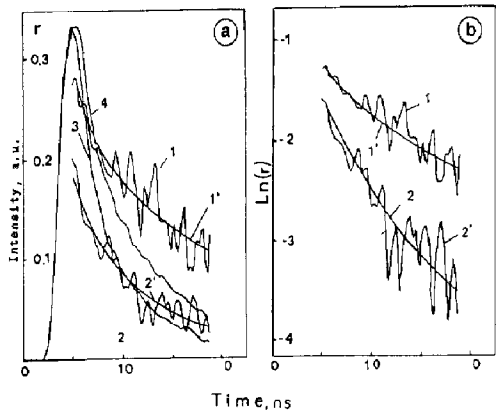

Fig. 8. Kinetics of emission intensity and anisotropy of 1-AN in phosphatidylcholine vesicles at 22 °C (excitation wavelength 395 nm). (a) The kinetics of anisotropy registered on the blue (430 nm, curve 1) and the red (475 nm, curve 2) slope of the fluorescence spectrum and its approximation by least-squares method (curves 1′ and 2′). Curves 3 and 4 represent the kinetics of fluorescence emission registered at the wavelength 430 and 475 nm, respectively. (b) The kinetics of emission anisotropy in the semilogarithmical scale registered at the wavelength 430 nm (curve 1) and 475 nm (curve 2) and its approximation (1′, 2′) by the least-squares method.

cated by the observed difference between the value of r_0 anisotropy measured at the initial moment and the limiting value r_0 of anisotropy (Fig. 7a, curves 1 and 2). This effect is more clearly pronounced at the red slope of the fluorescence spectrum (curve 2, Fig. 7). The experiments show that the subnanosecond component slows down on cooling of membrane suspension (Fig. 9). A similar result was obtained at the red-edge excitation of bilayer vesicles (Fig. 8). In particular at the excitation wavelength 395 nm the emission anisotropy kinetics also exhibit the dependence on the recording frequency. But in this case the initial value of anisotropy on the blue slope of the fluorescence spectrum appeared to be considerably higher and practically reaches the limiting value of $r_0 = 0.3$ (curve 1, Fig. 8). Generally it should be noted that the shift of the excitation wavelength from the blue to the red causes the continuous increase of the initial value of anisotropy up to the limiting value.

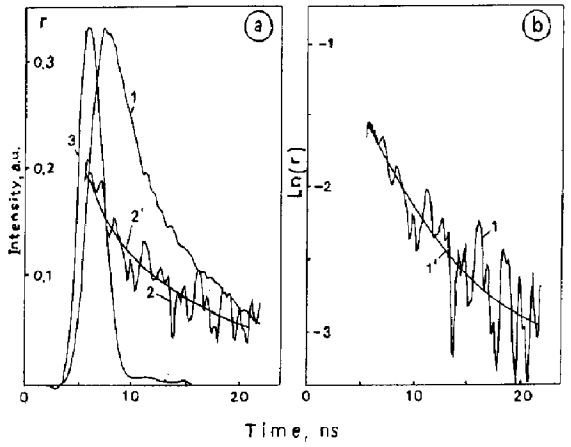

Fig. 9. Kinetics of emission intensity and anisotropy of 1-AN in phosphatidylcholine vesicles at 4 °C (excitation wavelength 337 nm, emission wavelength 430 nm). (a) The kinetics of fluorescence (curve 1), of emission anisotropy (curve 2) and the excitation pulse (curve 3). Curve 2 is the approximation of curve 2 by the least-squares method. (b) The kinetics of emission anisotropy in the semilogarithmical scale (curve 1) and its approximation by the least-squares method (1′).

4. Discussion

The comparative analysis of the results obtained for 1-AN in glycerol and vesicles proves the existence of inhomogeneous broadening of the electronic spectra of the probe in the solution and in the lipid bilayer membranes. In both systems the effect of red-edge excitation on the position of steady-state fluorescence spectra takes place. Besides, the time-dependent fluorescence shift occurs smoothly without any substantial change in the shape of emission spectra. At the same time two systems are characterized by different type of spectral relaxation. In particular, like in other polar solvents [19], the time-resolved spectra of 1-AN in glycerol attain the same limit independently on the excitation wavelength. In contrast to that for liposom suspension the limiting position of time-resolved fluorescence spectra considerably depends on the wavelength of excitation. This effect cannot be explained by the difference of viscosity in both systems because the microviscosity of bilayer at room temperature as estimated from probe rotations turned out to be even smaller than that of glycerol. This effect will be discussed below in Sections 4.4 and 4.5. Since the spectroscopic properties of 1-AN in egg lecithin vesicles and glycerol are similar, the analogy of the results obtained for the probe in the

solution and vesicles allows us to use the continuum spectroscopical model developed previously for of polar solutions for analysis of the properties of probe molecules in vesicles. However, the continuum model should be modified taking into account the specific structure of egg lecithin vesicles as a microheterogeneous system.

4.1 The model of polar solution

As is known, the fluorescence spectra of the probe are largely dependent on the polarity of the environment. In the case of fluorophore in solution, the role of the elementary unit determining the spectral properties plays the solvate (the fluorophore and its immediate environment). Rubinov and Tomin [20] considered the solution model which describes the solvate state by the action of two forces: the polarizing force caused by the interaction of a constant dipole moment of fluorophore molecule with surrounding media and the returning force caused by the interaction of the solvent molecule dipoles with reactive field R inside the solvate. The deviation of the solvate configuration from equilibrium increases its free energy compared to the minimum value corresponding to the equilibrium state by a value equal to the work done by the dipole to reconstruct the solvate.

In the differential form, the work dA done by the rigid dipole to polarize the environment by the value dR is:

$$dA = \mu\, dR \tag{1}$$

If we assume that the returning force is proportional to the reactive field strength, the ground-state solvate free energy will be described by the following equation:

$$F_g(R) = \left(R - R_g^{eq}\right)^2 / 2\mathscr{X} \tag{2}$$

where R_g^{eq} is reactive field strength in the equilibrium solvate, $\mathscr{X}$ is the solvent polarizability determined by the Clausius–Mossotti formula:

$$\mathscr{X} = \frac{\varepsilon - 1}{2\varepsilon + 1}\,\frac{2}{a^3} \tag{3}$$

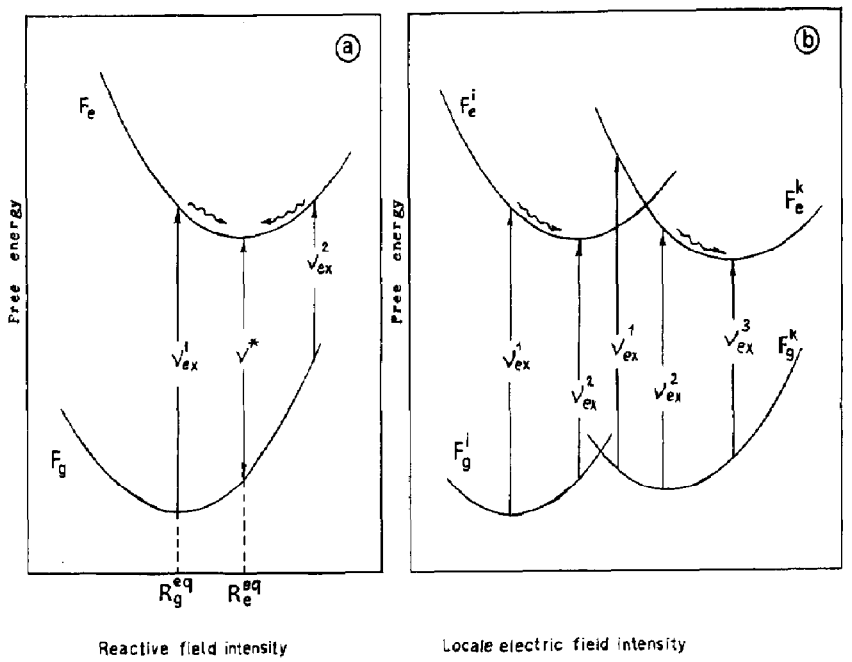

Fig. 10. The energy level diagram of fluorescence probe (field diagram). (a) Probe in polar solvent (no site-heterogeneity). (b) Probe in the system with site-heterogeneity. See explanation in text.

Here ε is the dielectric constant of the solvent, a is the Onsager sphere radius.

The excited solvate free energy is determined by a similar relation:

$$F_e(R) = (R - R_e^{eq})^2/2\mathscr{R} + h\nu_0 + \frac{\mathscr{R}}{2}(\mu_e + \mu_g)(\mu_e - \mu_g), \quad (4)$$

where ν_0 is the frequency of the pure electronic transition of the free probe molecule; h is the Planck constant; μ_g, μ_e are the dipole moments of the probe molecule in the ground and excited states and R_e^{eq} is the reactive field corresponding to the equilibrium excited state of the solvate.

The diagram of the solvate energy levels constructed according to eqs. (2) and (4) (field diagram) is given in Fig. 10a. It describes the dependence of the solvate free energy on the reactive field magnitude. For simplicity, the vibrational broadening of the electronic levels is not shown. The local solvate field R serves here as a generalized coordinate characterizing the state of the solvate. It varies due to the thermal fluctuation of the solution microstructure. Each point on the curves describing $F_g(R)$ and $F_e(R)$ corresponds to a particular type of solvate with the field R. Since the reactive field of the solvate has no time to change during the electronic transition (except for its electronic component which can be ignored), electronic transitions are represented in diagram by vertical arrows (intermolecular interpretation of the Franck–Condon principle).

Analysis of the diagram shows that when the excitation frequency corresponds to ν_{ex}^1 the process of solvate relaxation is expected to be followed by the red shift of the fluorescence spectrum. But if the excitation frequency is equal to ν_{ex}^2 the spectrum will be shifted in time towards the blue region. Between ν_{ex}^1 and ν_{ex}^2 there is a particular frequency ν^*, on excitation at which the solvate immediately find itself in the equilibrium state and, therefore, the spectrum relaxation does not occur. The dependence of the direction of time-resolved spectra shift on excitation frequency was first observed in [21].

An important result of this model is the Gaussian character of equilibrium distribution of solvates over the frequency of the pure electronic transition for absorption and emission:

$$\phi_{g,e}(\nu) = \frac{1}{\sqrt{2\pi}\sigma} \exp\left[-\frac{(\nu - \nu_{g,e}^0)^2}{2\sigma^2}\right], \quad (5)$$

where

$$\sigma = \frac{\mu_e - \mu_g}{2}\sqrt{\mathscr{R}kT}. \quad (6)$$

The frequency $\nu_{e,g}^0$ corresponds to the center of gravity of distribution and is equal to ν_{ex}^1 for absorption and ν^* for fluorescence, k is the Boltzmann constant, T is absolute temperature.

4.2 The model of the probe in membranes

The phospholipid bilayers which make up the membrane are arranged in such a way that the hydrophilic parts of phospholipids (charged heads) face the outside, whereas the hydrophobic parts (carbon chains) are located inside the bilayer. Owing to such organization, the membranes have a significant polarity gradient — the polarity decreases from the periphery to the center of the bilayer. The outer part of the membrane behaves as a polar solution, while its inner part is similar to a nonpolar solution. 1-AN molecules are uncharged and have a constant dipole moment, which allows their deep penetration into the membrane. As the incorporation of a probe into the membrane is a statistical process, a certain distribution of probes over depth must take place. Therefore the molecules must be situated in local electronic fields having different strengths. This results in statistical variation of the energy of intermolecular interactions, and, consequently, in inhomogeneous broadening of spectra. Besides, at each location of the probe fluctuation of the free energy is possible due to the segmentary dynamics of phospholipids to a change in the magnitude and direction of the local electric field of the membrane. At room temperature, the time of rotational diffusion of the probe is comparable with the lifetime of its excited state, and the translational motion of the probe is much slower than the rotational one.

Therefore, the inhomogeneous broadening associated with the segmentary dynamics of phospholipids and probe rotation has a dynamic character and manifests itself in the form of nanosecond spectral relaxation. On the other hand the inhomogeneous broadening associated with the distribution of probe over localization depth has a static character which manifests itself as a dependence of final position of time-resolved fluorescence spectrum on excitation wavelength (see Fig. 5).

The free energy diagram for the probe-environment centers (solvates) in egg lecithin vesicles plotted for simplicity for two different depths of probe location are shown on Fig. 10b. Here the local electric field serves as the generalized coordinate characterizing the states of the solvate. This parameter varies due to the fluctuation of the probe location depth and lipid segmentary motion. The free energy includes the electronic energy of the probe and the energy of the intermolecular interactions in the membrane solvate.

The free energy in each electronic state is represented by a curve with a minimum corresponding to a most stable probe-environment configuration in which all the electric forces determining the intermolecular interaction are compensated. In general, the equilibrium values of the local electric field differ for the ground and excited electronic states (g, e) owing to the difference of the electronic dipole moments μ_e and μ_g. It is well known that the frequency of optical transition is related to the electric field of solvate by the following equation:

$$\nu = \nu_0 - \frac{\Delta\mu}{h} E. \qquad (7)$$

where ν_0 is the frequency of electronic transition of a probe molecule in vacuum, $\Delta\mu$ is the change of the electric dipole moment on excitation, E is the value of the electric field, and h is Planck's constant. As follows from eq. (7), the energy gap between the ground and excited states tends to decrease with increasing solvate inner electric field, which, in turn, grows as the polarity of the environment increases. Therefore, the free energy curves in the left-hand part of the Fig. 10b correspond to the "blue" probe centers located closer to the membrane interior, while those in the right-hand part corresponds to the "red" centers located near the polar heads of the membrane.

Thus, the notion of dynamic inhomogeneous broadening holds for each membrane solvate, and its spectral properties can be analyzed by means of the field diagram for solution. Analysis of the spectral properties of the membrane system as a whole must take into account the heterogeneity of probe locations and can be carried out on the basis of more complicated diagram of Fig. 10b. In analyzing the diagram, it should be kept in mind that due to the low rate of probe translational motion at room temperature the transitions of the probe between differently located centers do not occur during the excited state lifetime. Therefore, the inhomogeneous broadening of the probe energy levels, associated with its different localization in vesicles, should be considered as a static one at room temperature.

4.3 Static inhomogeneous broadening of electronic spectra of the probe

As follows from the diagram (Fig. 10), a decrease of the excitation frequency in system with slow configurational relaxation (when emission occurs from the same configurational state of the solvate to which it was excited initially) should lead to a red shift of steady-state fluorescence. This phenomenon is observed in experiments in both solid and viscous solutions and in vesicles (Fig. 1). The well known temperature-dependent shift of fluorescence spectra (Fig. 2, curve1) has a complex character for 1-AN in vesicles: the monotonous function of temperature has a plateau in the range of 20–40 °C. This effect appears to be connected with the complex character of inhomogeneous broadening of electronic spectra of probes in the membrane. It is very likely that the position of the fluorescence spectrum maximum within the temperature interval of −20 to 20 °C depends on the rotational dynamics of the segments of phospholipids and of the probe, whereas, starting from 40 °C, the fluorescence spectrum maximum is additionally influenced by the probe translational motion. The

plateau on the temperature curve, observed within the 20–40 °C range, testifies to the fact that the configurational relaxation of the probe and segments of the membrane is already fast enough and does not affect the position of the maximum, while the role played by the probe translational motion within this range of temperature is insignificant.

4.4 Dynamic inhomogeneous broadening of electronic spectra of the probe

The use of time-resolved spectroscopy makes it possible to study the dynamics of configurational relaxation by observing the TDFS following optical excitation [12,22]. As follows from the diagram (Fig. 10a), the fluorescence spectrum relaxation in solutions depends essentially on the energy of excitation. Excitation at the maximum of absorption spectrum results in a long-wavelength temporal shift of time-resolved spectra. On transition to the red-edge excitation (towards the frequency ν^*, see Fig. 10a) the excess of free energy decreases which narrows the range of spectral relaxation. At the excitation frequency ν^* there is no spectral shift in time observed at all (see Fig. 5a).

TDFS also takes place for 1-AN in vesicles (Fig. 5b). But in this case the time-resolved spectra excited at the maximum and on the red slope of the absorption spectra relax to different positions. To explain such phenomenon, it should be assumed that the inhomogeneous spectral broadening caused by the statistical distribution of the probe over different locations in membrane is wider than the broadening caused by the fluctuations of solvate structure within the same location of the probe.

At such condition independently on frequency we excite the mixture of probe molecules, corresponding to different locations and different configuration states of solvate. It is clear that at higher frequency (blue excitation, arrow ν_1 at Fig. 10b) the solvates, situated at different ("red" and "blue") locations, appear to be mostly in non-equilibrium configurational states (i.e. most of the solvates are the "blue" ones). In this case the range of spectral shift during relaxation process is expected to be the largest one.

Let us consider another case, when the excitation frequency is decreased (arrow ν_2, Fig. 10a). In this case we obtain in the excited state the mixture of non-equilibrium ("blue") solvates in "red" locations and equilibrium ("red") solvates in "blue" location of the membrane. Evidently the range of the temporal shift in such case will be comparatively smaller. The decrease of spectral shift is clearly seen in Fig. 5b.

Thus, the inhomogeneous spectral broadening is caused by simultaneous effect of two different factors: (1) different locations of probe molecules in membrane and (2) different configurational states of solvates. During the process of relaxation (shift of spectrum in time) most of excited solvates become configurationally equilibrium and only the first reason of broadening is left. It follows form this that the different final position of fluorescence spectrum, observed at different excitation frequencies (see Fig. 5b), reflects the inhomogeneous broadening of probe spectrum exclusively due to the different locations of probe molecules in membrane.

4.5 Probe rotational dynamics in membrane and solution

Let us consider the diagram of probe energy levels in membrane (Fig. 10b). Excitation at the absorption band maximum by the frequency ν_1 is immediately followed by configurational relaxation during which a free energy excess is released in the solvate. This may produce local "heating" of the solvate which is able to accelerate the probe rotation, producing additional fluorescence depolarization. During relaxation the time-resolved spectrum is shifted to longer wavelengths and the magnitude of the additional depolarization must therefore be greater at the long-wave part of the fluorescence spectrum. We observed this phenomenon experimentally for 1-AN in phospholipid membranes (curves 2,2′ in Figs. 7 and 8). It is interesting to notice that the registered initial anisotropy is considerably smaller than the limiting value. This indicates that at excitation by the wavelength 337 nm the

subnanosecond (nonresolved in our experiment) depolarization takes place. The possibility of the effect of the excitation wavelength on the limiting anisotropy must be excluded because the time-resolved values of 1-AN anisotropy at excitation at 337 nm in cooled vesicles (Fig. 9) and in glycerol (Fig. 6) are close to the limiting anisotropy.

The discussed data confirm that the additional rotation of the probe during the relaxation period depends on the amount of released free energy. At red-edge excitation (395 nm) the excess of the released free energy becomes small as shown by TDFS measurements (Fig. 5) and the subnanosecond depolarization disappears (Fig. 8). Yet additional fluorescence depolarization still takes place (curve 2, Fig. 8). These results show that in the course of configurational relaxation the dipole–dipole interaction energy excess goes to rotational degrees of freedom of probe.

Such an effect can be regarded as light-induced molecular rotation and it was observed earlier in a polar solution of 3-amino-*N*-methylphthalimide [23]. We have analyzed the thermal regime of solvates of this system (glycerol solution of 3-amino-*N*-methylphthalimide at room temperature) which spectral and polarization properties have been studied in detail by us [24]. It was shown that the dissipation time of thermal fluctuations in this case was equal approximately to 4 ps. Then at the configurational relaxation time about 1 ns and spectral shift of 3700 cm^{-1} the change of the solvate temperature correspond to 50 °C [24].

More likely the phenomenon of light-induced rotation of molecules is a universal one and should be taken into account when considering the spectroscopic and photochemical properties of different liquid polar systems which include dye molecules with inhomogeneous broadening of electronic spectra. The peculiarity of light-induced rotation of the probe in the membrane is connected with its specific structure, in particular, with rigid arrangement of phospholipid molecules in the bilayers. It appears that the probe itself is more mobile than surrounding lipid segments. The absence of light-induced rotation of 1-AN in glycerol is likely to be associated with the realization in the solution of the stick boundary condition [25]. Using the Einstein formula, we find from the rotational time of the 1-AN in glycerol that the probe solvation volume is $V = 0.6$ nm^3, which is three times higher than the geometrical volume of the 1-AN molecule. On the other hand, the solvation volume of 3-amino-*N*-methylphthalimide in glycerol, where light-induced rotation takes place [23,24], is equal to $V = 0.1$ nm^3, which correspond to the geometrical volume of this molecule. Therefore, we suggest that this effect occurs in molecular systems in which the configurational relaxation includes not only the rotational motion of solvent molecules, but the probe molecules reorientation as well.

Lakowicz [26] suggested that in the course of relaxation the interaction energy is increased and this should result in retarding the chromophore rotation. A similar model of "solvate coat" was considered by Gaisenok and Sargevski [25]. This model could suggest the slower rotation of the "red" (long-wavelength emitting) species. However, we observed opposite effect: in the course of transformation of "blue" into "red" species the rotation is accelerated. Similar results were reported for 3-amino-*N*-methylphthalimide in glycerol [23] where the dependence of time-resolved anisotropy on excitation and emission wavelength was clearly observed. Thus, at spectral relaxation shift to longer wavelengths (excitation at maximum) the anisotropy values appear to be higher on the blue slope of emission spectrum. Correspondingly in the case of relaxation to shorter wavelengths (far red-edge excitation) the time-resolved anisotropy values become higher on the red slope. Such a specific dependence of time-resolved anisotropy spectrum on the excitation wavelength is in full accordance with our model (Fig. 10a).

It should also be stressed that the time-resolved anisotropy values measured in our experiments are not affected by the non-exponentiality of the emission decay at fixed wavelengths connected with the temporal shift of the spectrum. However, such an effect in significant in the case of steady-state anisotropy measurements, as was shown by Bakhshiev and coworkers [27].

Ludescher et al. [28] considered the behavior of time-resolved anisotropy in heterogeneous sys-

tem where two distinct fluorophore types have rotational correlation times τ_{rot1} and τ_{rot2} without interconversion between them. As to this model it does not permit to explain the data obtained in this work. On the one hand, we have found that r_0 is independent of the excitation frequency within the long-wave absorption band and on the other hand the excited state lifetime does not essentially depend on the excitation frequency [29]. Then, from the point of view of this model, we must assume that both types of centers, the red and the blue one, have equal r_0 and quite close lifetimes. Besides, we must assume that τ_{rot1} is greater than τ_{rot2} (this follows from the dependence of the emission anisotropy kinetics on the registration frequency). Then, at the red edge excitation the anisotropy must decrease, which contradicts our experimental data.

Dependence of the rotational rate of the probe in membrane upon the configurational energy of the probe makes more complicated the determination of membrane microviscosity by the Perrin equation. Since this equation does not take into account the effect of light-induced rotation of molecules. For the determination of microviscosity the rotational correlation time should be obtained from such an experiment which is not effect by the light-induced rotation of the probe. In particular correct data may be obtained if the determination of rotational time is carried out after the completion of the relaxational process. Besides, it could be important that at the red-edge excitation the photoselection between different chromophore locations occurs and we may obtain microviscosity of the more polar part of the membrane where most of the long-wave emitting centers are located. For centers of such kind using this approach we obtained the value of rotational correlation time for 1-AN in phosphatidylcholine membrane equal to 18 ± 2 ns.

5. Conclusions

(1) The electronic spectra of 1-AN in phospholipid bilayer membranes show considerable inhomogeneity. Unlike solutions there are two reasons for inhomogeneous broadening. The first is connected with different locations of probe molecules in the membrane. Inhomogeneous broadening due to the first factor has a steady-state character. The second reason is similar to that of solution and linked with fluctuations of solvate structure. This type of broadening has a dynamic character.

Inhomogeneous broadening affects significantly the spectroscopic properties of the 1-AN probe in bilayer phospholipid membranes, such as the red-edge excitation fluorescence shift of the steady-state emission spectrum, the nanosecond kinetics of fluorescence spectra, the dependence of the time-resolved spectra position on the excitation wavelength.

(2) The process of spectral relaxation is accompanied by the release of the intermolecular interactions energy excess, which results in light-induced rotation of the probe. This process causes the rapid subnanosecond kinetics of fluorescence anisotropy and explains its non-exponential character. As a consequence of the specific dependence of fluorescence depolarization rate on the excitation and emission wavelength is observed. The effect of light-induced rotation of the probe is most pronounced when the recording is carried out at the long-wave of the fluorescence spectra and the excitation is made near the absorption maximum. It vanishes at the red-edge excitation.

(3) The revealed inhomogeneous broadening of electronic spectra and the effect of light-induced rotations must take place in a considerable number of biological systems. A study of these phenomena could be important for obtaining new data about their structure and dynamics.

References

1 Yu. A. Vladimirov and G.E. Dobretsov, Fluorescent probes in the study of biological membranes (Nauka, Moscow, 1980) p. 320.
2 J.R. Lakowicz, Principles of fluorescent spectroscopy (Plenum Press, New York, NY, 1983).
3 F. Grieser and C.J. Drummond, J. Phys. Chem. 82 (1988) 5580.
4 J. Slavik, Biochim. Biophys. Acta 694 (1982) 1.
5 L. Brand and J.R. Gohlike, Annu. Rev. Biochem. 41 (1971) 843.

6 N.G. Bakhshiev, Spectroscopy of intermolecular interactions (Nauka, Leningrad, 1972) p. 263.
7 A.P. Demchenko and N.V. Shcherbatska, Biophys. Chem. 22 (1985) 131.
8 G.K. Radda and J. Vanderkooi, Biochim. Biophys. Acta 265 (1972) 509.
9 E.D. Matayoshi and A.M. Kleinfeld, Biochim. Biophys. Acta 644 (1981) 233.
10 C.M. Colley and J.C. Metcalf, FEBS Lett. 24 (1972) 241.
11 P. Ting and A.K. Solomon, Biochim. Biophys. Acta 406 (1975) 447.
12 M.G. Badea, R.P. DeToma and L. Brand, Biophys. J. 24 (1978) 197.
13 D.M. Gakamsky, A.P. Demchenko, N.A. Nemkovich, A.N. Rubinov, V.I. Tomin and N.V. Shcherbatska, Time-resolved laser spectroscopy of 1-AN probe in phospholipid membranes (Preprint No. 487 Institute of Physics of the BSSR Academy of Sciences, Minsk, USSR, 1987) p. 29.
14 N.V. Shcherbatska and A.P. Demchenko, Biophysika (USSR) 34 (1989) 574.
15 D.M. Small and M.C. Bourger, Biochim. Biophys. Acta 125 (1966) 563.
16 Yu. N. Levchuk, Z.N. Volovik and N.V. Shcherbatska, Ukrain. Biochim. J. (USSR) 55 (1983) 191.
17 C.L. Bashford, C. Morgan and G.K. Radda, Biochim. Biophys. Acta 298 (1973) 1015.
18 D.M. Gakamsky, N.A. Nemkovich, A.N. Rubinov, V.I. Tomin and E.V. Tchaykovski, Kvantovaya Electron. (USSR) 13(1986) 2271.
19 V.I. Tomin and A.N. Rubinov, Zhurnal Prikl. Spectrosk. (USSR) 35 (1981) 236.
20 A.N. Rubinov and V.I. Tomin, Inhomogeneous broadening of electronic spectra of dye molecules in solutions (Preprints No. 525 and No. 536, Institute of Physics of The BSSR Academy of Sciences, Minsk, USSR, 1988) p. 43 and p. 30.
21 N.A. Nemkovich, V.I. Matseiko, A.N. Rubinov and V.I. Tomin, Pisma Zh. Eksp. Teor. Fiz. (USSR) 29 (1979) 780.
22 M. Maroncelli and G.R. Fleming, J. Chem. Phys. 86 (1978) 6221.
23 D.M. Gakamsky, N.A. Nemkovich, A.N. Rubinov and V.I. Tomin, Opt. Spectrosk. (USSR) 64 (1988) 678.
24 D.M. Gakamsky, N.A. Nemkovich, A.N. Rubinov and V.I. Tomin, J. Mol. Liquids. 45 (1990) 33. D.M. Gakamsky, N.A. Nemkovich, A.N. Rubinov. 1989. Izv. AN SSSR, Ser. Fiz. (USSR) 53 (1989) 2396; D.M. Gakamsky, N.A. Nemkovich, A.N. Rubinov, Springer Proceedings in Physics. 49 (1990) 270; D.M. Gakamsky. N.A. Nemcovich, A.N. Rubinov, Zhurnal Prikl. Spectrosk. (USSR) 54 (1991) 183.
25 V.A. Gaisenok and A.M. Sargevski. Absorption and fluorescence anisotropy of complex molecules (University of Minsk, Minsk, USSR, 1986) p. 316.
26 J.R. Lakowicz, Biophys. Chem. 19 (1984) 13.
27 Yu. T. Mazurenko, N.G. Bakshiev and Piterskaya, Opt. Spektrosk. (USSR) 25 (1968) 92.
28 R.D. Ludescher, L. Peting, S. Hudson and B. Hudson, Biophys. Chem. 28 (1987) 59.
29 D.M. Gakamsky, A.A. Goldin and A.N. Rubinov, Biophys. Chem. (submitted).